SOME CONSIDERATIONS ON NEUTRINO FACILITIES WITH LARGE ACCELERATORS

C. A. Ramm
CERN

1.1. Neutrino Parents

High energy neutrino fluxes of experimental abundance have been obtained from the muon decay of pions and kaons:

$$\pi^{\pm} \longrightarrow \mu^{\pm} + (\nu_{\mu},\ \bar{\nu}_{\mu}),$$
$$K^{\pm} \longrightarrow \mu^{\pm} + (\nu_{\mu} + \bar{\nu}_{\mu}).$$

The short lifetimes, the branching ratios and the two-body decay are particularly favourable for neutrino production. Of the other less prolific parents the muons and $K_{\beta 3}$ contribute to the flux, especially as sources of electron neutrinos:

$$\mu^{\pm} \longrightarrow e^{\pm} + (\nu_e,\ \bar{\nu}_e) + (\nu_{\mu} + \bar{\nu}_{\mu}),$$
$$K^{\pm} \longrightarrow e^{\pm} + \pi^0 + (\nu_e,\ \bar{\nu}_e).$$

Both are three-body decays, and thus give softer neutrino spectra. They will not be considered here.

1.2. Neutrino Fluxes from Two-Body Decay of Relativistic Parents

Suppose an isotropic source of parents (Fig. 1). From symmetry, and the divergence theorem,

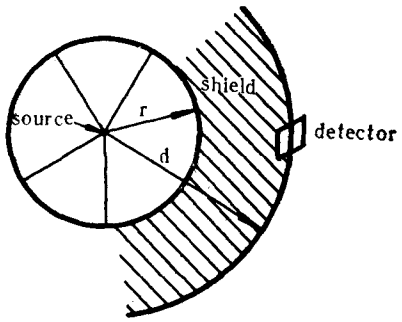

Fig. 1.

the flux of neutrinos per unit surface of spherical shell at radius d, per parent, per steradian, is

$$n_1 = \frac{r}{\lambda d^2},$$

if $\lambda \gg r$, and there is one neutrino per parent decay. For two-body decay from relativistic parents the mean neutrino energy $\bar{E}_{\nu}$ is

$$\bar{E}_{\nu} = \gamma E'_{\nu},$$

where E'_{ν} is the neutrino energy in CS.

In some practical situations the parent flux is of nearly uniform density over a cone of

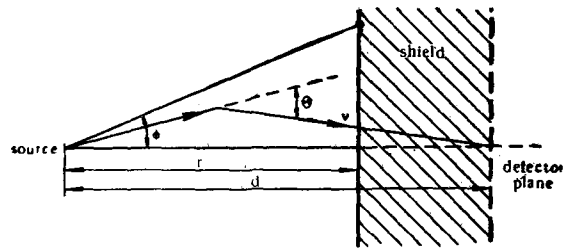

Fig. 2.

small semi-angle (Fig. 2). The axial neutrino flux in the detector plane, per parent in this cone ($\lambda \gg r$) can then be shown to be [1]

$$n_2 = \frac{\gamma^2}{\pi\lambda d}\frac{1}{\gamma\Phi}\tan^{-1}\frac{r\gamma\Phi}{(1+\gamma^2\Phi^2)d - r},$$

which gives the distribution of Fig. 3. The average energy of the axial neutrino flux for these conditions is

$$\bar{E}_{\nu} = \frac{1}{n}\int E_{\nu}(\Phi,\ r)\frac{dn}{dr}dr =$$
$$= \gamma E'_{\nu}\left\{2 - \frac{\gamma^2\Phi^2\,(d^2 + (d-r)^2 + 2\gamma^2\Phi^2 d^2)}{2\,(1+\gamma^2\Phi^2)\,[(d-r)^2 + \gamma^2\Phi^2 d^2]}\right\}$$

which is shown in Fig. 4. In the limit for $\gamma^2\Phi^2 \gg 1$ then $\bar{E}_{\nu} = \gamma E'_{\nu}$, and for $\gamma^2\Phi^2 \ll 1$ the average neutrino energy tends to the maximum value $2\gamma E'_{\nu}$.

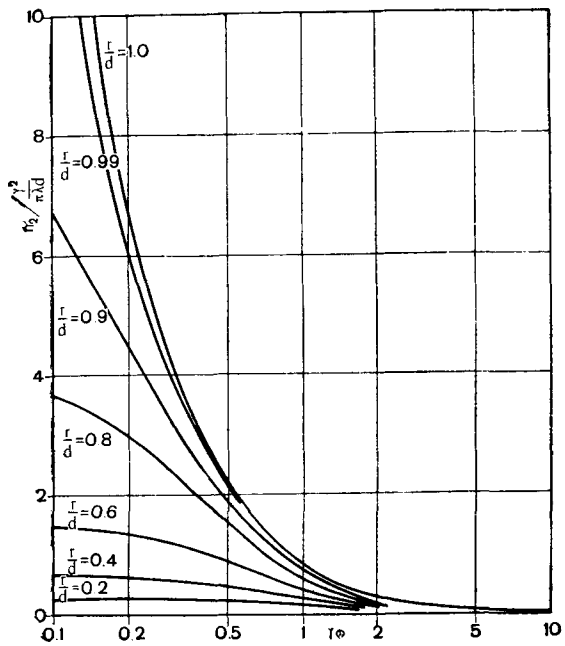

Fig. 3.

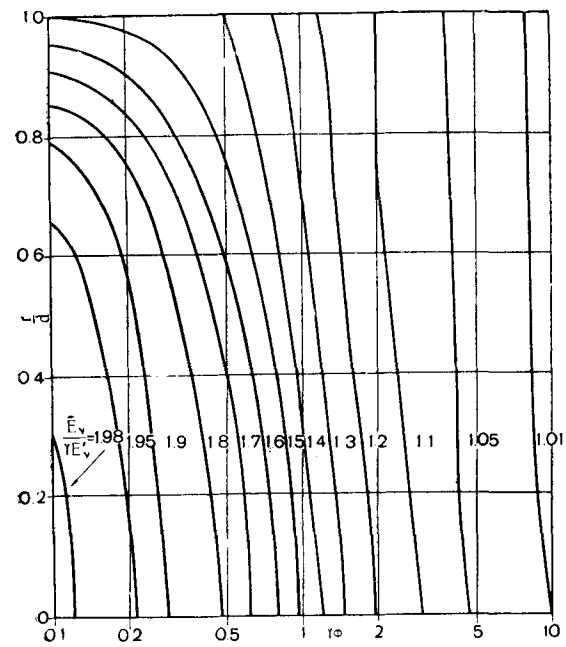

Fig. 4.

For a pencil beam (Fig. 5) the mean neutrino flux per unit area, within a radius y of the point of intersection of the pencil with the detector plane for a pencil of decay length x, is

$$n = \frac{\gamma^2}{\pi\lambda d} \cdot \frac{d}{\gamma y} \tan^{-1} \frac{x\gamma y}{\gamma^2 y^2 + d(d-x)},$$

which is the same relation as Fig. 3, with the substitution $\Phi = \frac{y}{d}$ and $x = r$. The mean

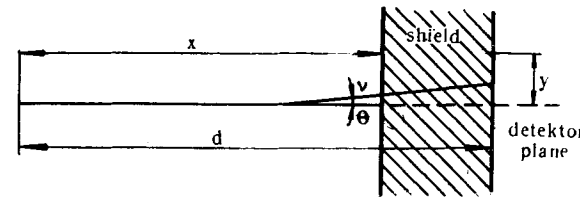

Fig. 5.

energy of the neutrinos within the circle of radius y is

$$\bar{E}_\nu = \frac{1}{n} \int E_\nu(x) \frac{dn}{dx} dx =$$

$$= \gamma E'_\nu \left\{ 2 - \frac{\gamma^2 y^2 (d^2 + (d-x)^2 + 2\gamma^2 y^2)}{2(d^2+\gamma^2 y^2)[(d-x)^2+\gamma^2 y^2]} \right\},$$

which is the same as the relation shown in Fig. 4, with the preceding substitutions. It can be shown that, for the same decay length and shielding, the contribution to the neutrino flux at the axis, from one parent: in the cone of small semi-angle Φ, is equal in intensity and energy distribution to the total neutrino flux, within the circle of radius $\gamma\Phi d$, from a single axial parent. The neutrino flux per unit area at a radius y is

$$N(y) = \frac{1}{2\pi y} \frac{dx}{dy} = \frac{\gamma}{2\pi\lambda y} \left\{ \tan^{-1} \frac{x\gamma y}{\gamma^2 y^2 + d(d-x)} + \right.$$

$$\left. + \frac{x\gamma y (d^2 - dx - \gamma^2 y^2)}{(d^2+\gamma^2 y^2)[(d-x)^2+\gamma^2 y^2]} \right\},$$

which is shown in Fig. 6 from which it will be seen that the intensity falls rapidly for $\gamma\Phi \gg 1$. The mean neutrino energy of the flux at radius y is

$$\bar{E}_\nu = \frac{2\gamma^3 E'_\nu}{\pi\lambda N(y)} \left\{ \frac{(d-x)[5(d-x)^2+3\gamma^2 y^2]}{8[(d-x)^2+\gamma^2 y^2]^2} - \right.$$

$$- \frac{d(5d^2+3\gamma^2 y^2)}{8(d^2+\gamma^2 y^2)^2} +$$

$$\left. + \frac{3}{8\gamma y} \left(\tan^{-1} \frac{d}{\gamma y} - \tan^{-1} \frac{d-x}{\gamma y} \right) \right\},$$

which is shown in Fig. 7. By combining the preceding results, together with the energy

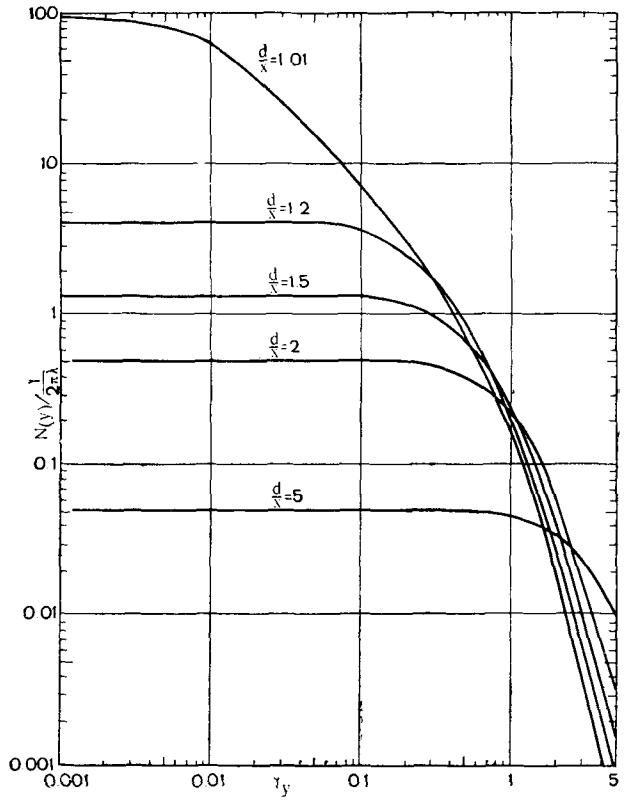

Fig. 6.

and angular distribution of the parents, it is possible to determine the neutrino flux distribution from a given experimental layout.

1.3. Parent Spectra from 25 GeV Protons

In the design of the CERN neutrino experiment [2] the parent spectra from the smoothed experimental results from the PS [3] and the AGS [4] for pion and kaon production were used to determine the spectra chown in Figs. 8, 9, 10.

It appears that the density of parents is uniform over a certain range of small angles, but there are no published data in the forward direction. In any case the production extends far beyond the cone $\lambda\Phi = 1$, and thus, especially for pions, the importance of parent focusing to increase the energy and intensity of the axial neutrino flux, is evident from the results of the preceding section.

1.4. Extrapolation to Higher Energy

Various formulae have been proposed for the extrapolation of observed production spectra at 25—30 GeV to machines of much higher energy, based largely on the cosmic ray evidence that the average transverse momentum

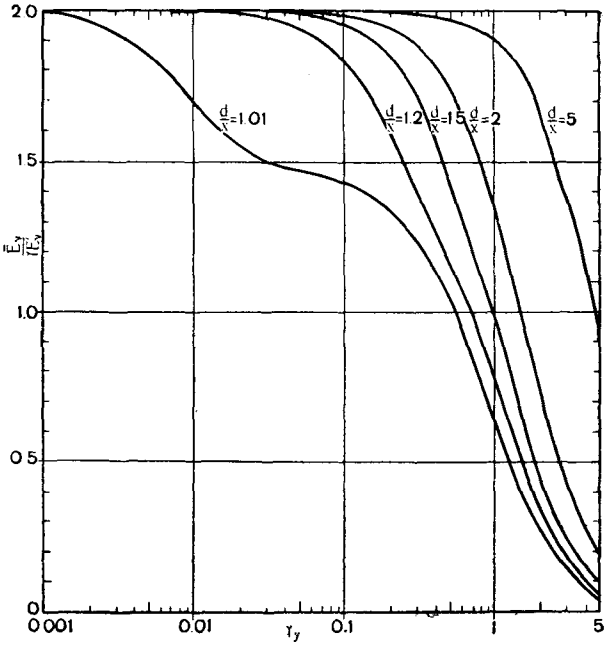

Fig. 7.

in secondary particle production appears to be independent of primary energy. Of these, the Cocconi, Perkins, Koester [5] formula represents the experimental data only at low energies, the von Dardel [6] formula for the forward direction falls identically on Hagedorn's [7] predictions and fits the reported experimental results for pions.

If these formulae are used for the prediction of pion spectra at much higher energies, they lead to somewhat different results. It is not known how the kaon spectra may be extrapolated other than by a postulate of a constant pion to kaon ratio.

However, it follows that if in the secondary production from very high energy protons the average transverse momentum is constant, and independent of secondary energy, a focusing factor is required which is constant for each type of secondary. Suppose the secondary production of momentum p_s

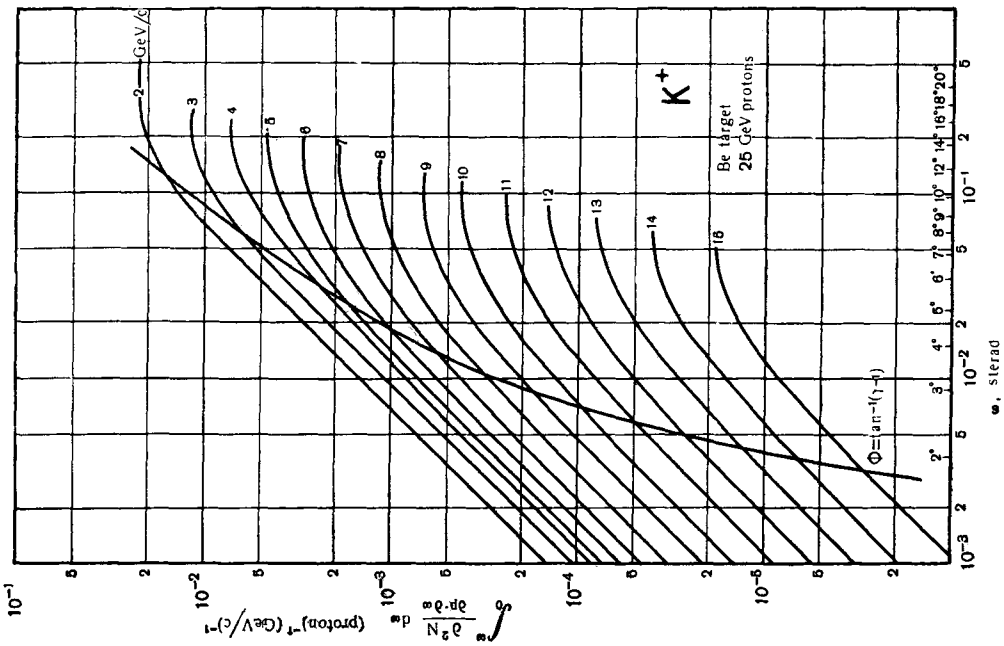
K+
Be target
25 GeV protons
GeV/c
Θ=tan⁻¹(1-η)
ω, sterad
(proton)⁻¹ (GeV/c)⁻¹

Fig. 9.

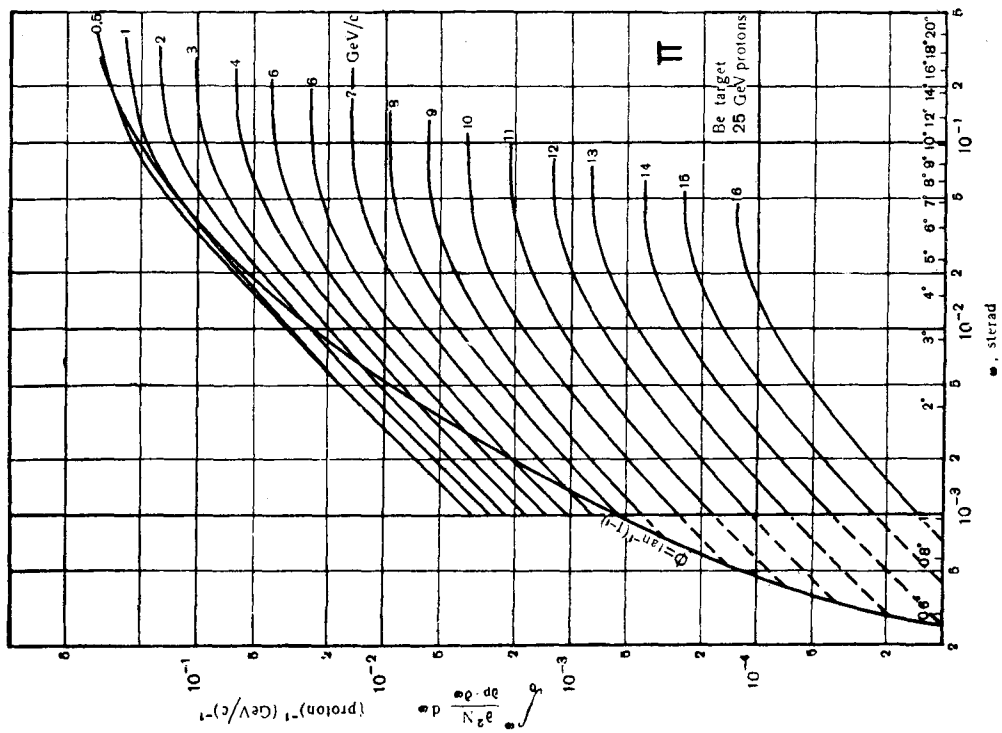
π
Be target
25 GeV protons
GeV/c
Θ=tan⁻¹(1-η)
ω, sterad
(proton)⁻¹ (GeV/c)⁻¹

Fig. 8.

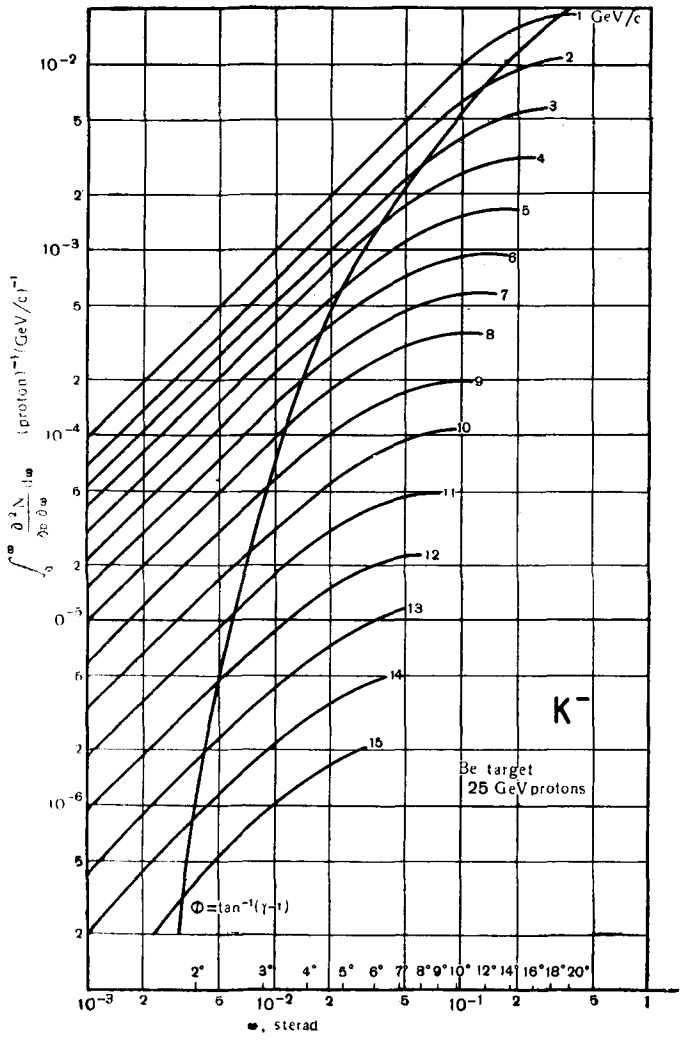

Fig. 10.

is contained in some cone of semi-angle Φ. Then $\Phi \sim \frac{\bar{p}_\perp}{p_s}$ and for the cases we consider $p_s \sim E_s$, hence

$$\gamma\Phi \sim \frac{\bar{P}_\perp}{m_s} .$$

Thus for pions, the assumed secondary production extends to $\gamma\Phi \sim 7$ and for kaons to $\gamma\Phi \sim 2$, whereas for efficient axial neutrino production, and shielding thickness equal to about the decay length, Φ should be appreciably less than γ^{-1}. Hence, the need for a constant factor of compression of the secondary production cone, independent of secondary energy, but about inversely proportional to parent rest mass.

2. EXPERIMENTAL LAYOUTS

2.1. Parents

The most numerous neutrino parents from accelerators are pions and kaons, which give predominantly fluxes of muon neutrinos. High energy electron neutrino fluxes have not yet been exploited, but experiments are possible with electron neutrino fluxes from both these and other parents. The advantages of focusing have already been discussed, and it has been shown in 1.2 that for parent beams of small divergence the neutrinos from pions are confined within a cone of about one third the semi-angle as that of neutrinos of the same energy from kaons. Some spatial separation between pion-kaon neutrino fluxes can thus be achieved.

In the present neutrino experiment a magnetic horn [8] has been used to direct a certain energy band of the parents towards the neutrino detectors, with appropriate enhancement of the neutrino flux [9] over that which could be obtained from a simple target alone. The resultant spectrum is included in Fig. 11. In principle the most intense neutrino fluxes are obtained for pencil focusing of the parents, which is approximated over a certain momentum band by the magnetic horn. It is possible to imagine arrangements which would be closely equivalent to pencil focusing, Fig. 12 is one example, and which would have certain advantages to be discussed shortly.

2.2. Shielding

In the recent experiments [2, 10] the shielding thickness has been chosen to absorb all muons from pion decay. Experimental data for muon scattering exists from cosmic ray studies [11, 12] and from experiments at the Bevatron [13]. Since the mean free-path for large angle muon scattering is long, the energy loss is mainly by ionization, and thus for the design of shieldings it is possible to arrive at simple graphical representations. Iso-absorption and iso-$p\Phi$ diagrams have been construc-

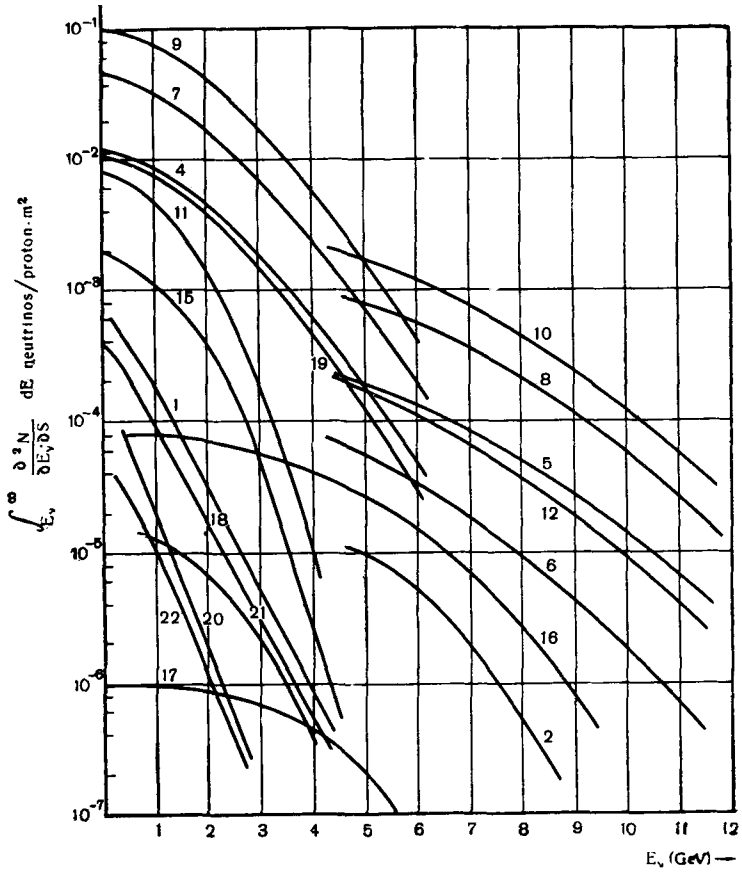

Fig. 11. Neutrino fluxes from 25 GeV protons on Be target.

Axial neutrinos from natural parent spectrum, no target absorption. (r = 25 M, d = 50 M).
Curve 1. From pions of either sign.
Curve 2. From positive kaons.
Axial neutrino flux from pencil focused parents, no target absorption (x = 25 M, d = 50 M).
Curve 4. From pions of either sign.
Curve 5. From positive kaons.
Curve 6. From negative kaons. (x = 10 M, d = 50 M).
Curve 7. From pions of either sign.
Curve 8. From positive kaons (x = 5 M, d = 50 M).
Curve 9. From pions of either sign.
Curve 10. From positive kaons.
The negative kaon curves for x-10 M and x = 5 M have the same displacements as the positive kaon surves.
Neutrino flux averaged over circle of diameter 1 M from pencil focused parents, no target absorption (x=25 M, d = 50 M).
Curve 11. Pions of either sign.
Curve 12. Positive kaons.
From comparison the following curves have also been included: From computations [9] of S. van der Meer [r=23.5 M, d=48.25M).
Neutrino flux with magnetic horn at 300 kA, with adsorption.
Curve 15. From focused pions.
Curve 16. From focused positive kaons.
Curve 17. From defocused kaons.
Neutrinos with magnetic horn at zero current, with absorption.
Curve 18. From pions.
Pencil focused parents, without absorption.
Curve 19. From pions.
Curve 20. Neutrinos from pions in the Brookhaven-Columbia-experiment [10].
Curve 21. Neutrinos from kaons in the Brookhaven-Columbia-experiment [10].
Curve 22. Neutrinos from pions in the first CERN experiment.
N o t e: Curves 2, 5, 6, 8, 10 and 12 have not been computed below 5 GeV.

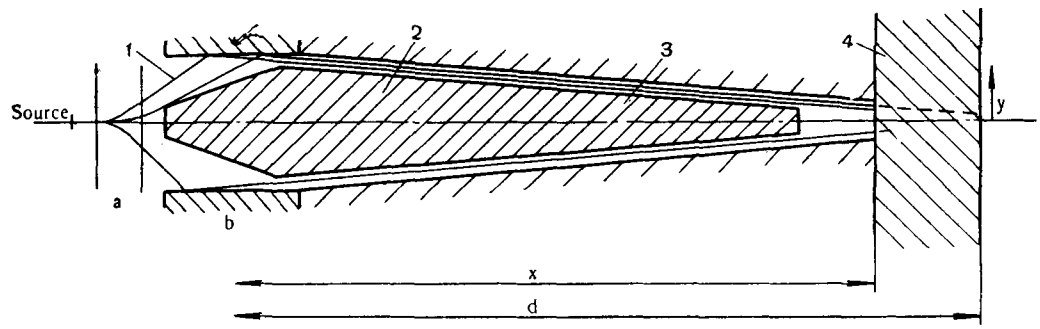

Fig. 12. Principle of neutrino production from parent pencil (Not to scale):
a — magnetic diverging region; *b* — region of magnetic «reflector» (for useful parents); *1* — neutrino parents; *2* — high energy muon shield; *3* — decay path; *4* — shielding.

ted to give visual appreciation of the relative merits of different shielding layouts. Examples of these lines are shown in Fig. 13. Since the muons have closely the direction of their parents, the origin of all primary muons may, with sufficient approximation, be taken to be the target. Under these circumstances the most efficient use of shielding is to have two components, the main core at the end of the parent decay path, and a funnel, close to the target, to cast a shadow outside of the decay path.

It is expected that the muon straggling [14] increases slowly with energy and thus the extra

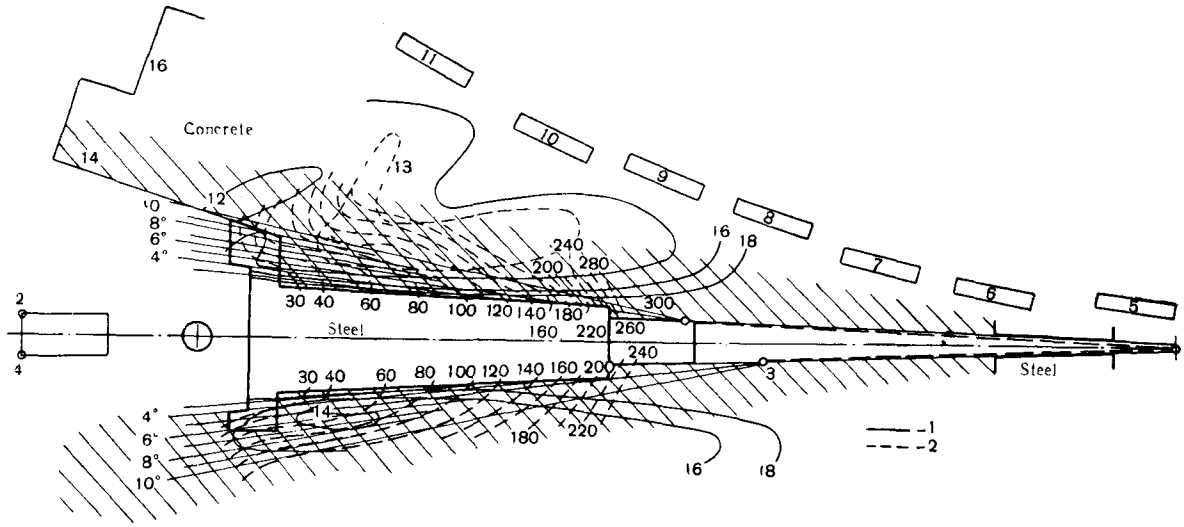

Fig. 13. Principles of muon shielding for steel core immersed in concrete. Upper lines for signle scatter from 1 to 2, lower lines for signale scatter 3 to 4:
1 — iso-absorption regions (meters of steel equivalent); *2* — iso-$p\Phi$ regions (GeV/c x degrees).

shielding necessary to account for it must also increase with parent energy. The calculated Gaussian and Landau [15] straggling are shown in Fig. 14, which gives the probability per metre of a muon having greater than the average range in iron packed to 7.0 g·cm^{-2}. In the type of layout of Fig. 13, the shielding thickness is governed by muons from a class of parents which makes no useful contribution to the neutrino flux. If it were possible to introduce a momentum cut-off in the parent spectra the layout could be shortened and the intensity of the neutrino flux increased correspondingly. It may be possible to achieve such an arrangement by the focusing of Fig. 12 where only those parents of momentum less than a certain limiting value would be returned by the reflector, and hence the shielding thickness would be fixed by these.

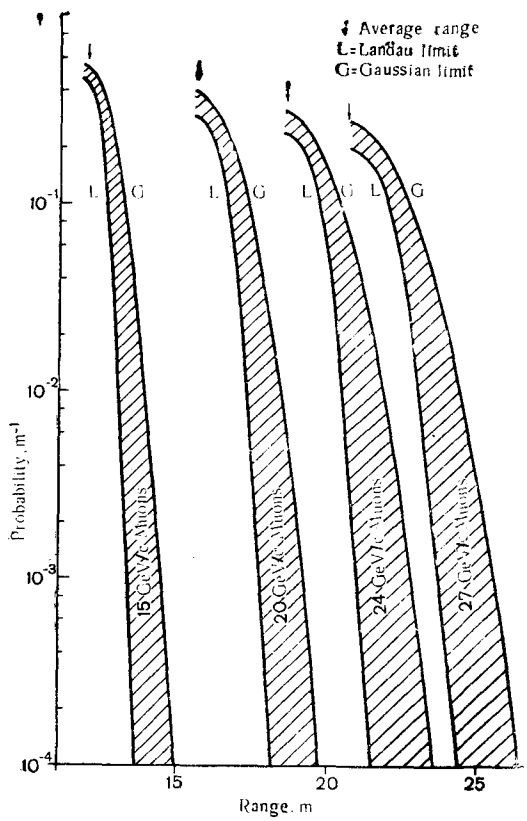

Fig. 14.

It is possible also to imagine the use of magnetized iron shieldings, and to some extent, of heavier shielding material than iron which has proviosly been used, although the specific stopping power for muons increases more slowly than the density on account of a Z dependence in the ionization loss. Possible improvements which might be achieved in principle in the differential spectrum in the present experiments, are shown in Fig. 11.

Since the neutron interaction cross-section is almost independent of energy above 1 GeV the neutron shielding considerations are relatively inderendent of accelerator energy. The basic muon shielding shown in Fig. 13 must be strengthened in direction perpendicular to

the axis to reduce the stray neutron background to a tolerable level. There will remain always, however, a certain residual flux of particles due to neutrino interactions in the shielding material itself.

2.3. Detectors

As a consequence of the cross-sections involved in neutrino interactions, detectors are inevitably massive, in the previously reported experiments spark chambers of tens of tons have been used, and in the present experiments a bubble chamber with 0.75 ton of working fluid and some 80 t of spark chambers are used. The neutrino flux is unattenuated except by geometry, and thus the detector may be imagined as a window by which the interactions in the path of the neutrinos are made visible, a feature which may be used to increase the information obtainable from the experiments, since the flux of product particles from neutrino interactions in material surrounding the detectors may be similar to that produced directly in the detectors. It is not the present purpose to discuss the detectors themselves.

REFERENCES

1. Ramm C. A. Neutrino Spectra from the Two-Body Decay of Relativistic Parents. CERN NPA Seminars, 1963.
2. To be published.
3. Diddens A. N., Lillethun E., Manning G., Taylor A. E., Walker T. G. and Wetherell A. M. Data on Negative Particle Spectra, CERN (unpublished).
4. Baker W. F., Cool R. L., Jenkins E. W., Kycia T. F., Lindenbaum S. J., Love W. A., Lüers D., Niederer J. A., Ozaki S., Read A. L., Russell J. J. and Yuan L. C. L. Phys. Rev. Lett., 7, 101 (1961).
5. Cocconi G., Koester L. J. and Perkins D. H. Calculation of Particle Fluxes from Proton Synchrotrons of Energy 10—1000 GeV; UCID-1444, UCRL-SS 28-2 (1961).
6. von Dardel G. CERN NP/Int. Report 62-17, Oct. 1962.
7. von Behr J. and Hagedorn R. CERN 60-20.
8. Giesch M., Kuipen B., Langeseth B., van der Meer S., Neet D., Plass G., Pluym G. and de Raad B. Nucl. Instrum. and Methods, **20**, 58 (1963).
9. van der Meer S. and Vahlbruch K. M. CERN NPA/Int. 63-11, May 1963.
10. Danby G., Gaillard J. M., Goulianos K., Lederman L. M., Mistry N. B., Schwartz M. and Steinberger J. In: Proceedings of the International Conference on High Energy Physics (CERN, 1962), p. 809.
11. Diddens A. N., Lillethun E., Manning G., Taylor A. E., Walker T. G. and Wetherell A. M. Phys. Rev. Lett., **9**, 32 (1962).
12. Fowler G. N. and Wolfendale A. W. In: Progress in Flementary Particle and Cosmic Ray Physics IV, 1958, p. 107.
13. Fukui S., Kitamura T. and Watase Y. Phys. Rev., **113**, 315 (1959).
14. Kim C. Y., Kaneko S., Kim Y. B., Masek G. E. and Williams R. W. Ibid., **122**, 1641 (1961).
15. Sternheimer R. M. Ibid., **117**, 485 (1960).
16. Landau L. D. J. Phys. of USSR, 8, 201 (1944).

DISCUSSION

N. A. Burgov

How was the divergence of the particle beam creating neutrinos reduced?

C. A. Ramm

The magnetic horn designed by Dr. van der Meer, who is at the conference, consists of two conical coaxial current carrying conductors. Neutrino parents are concentrated by the azimuthal field between them.

A. K. Val'ter

I would like a more detailed explanation of the operating principles of the device for neutrino experiments indicated by one of the slides and distinguished by the conical configuration of the outer shield by the presence of an external "neck" in the form of a body of revolution and a relatively narrow and long gap between the two shielding portions.

C. A. Ramm

The principle is that the central shielding would absorb high energy muons, from parents not deviated by the diverging field. Useful neutrino parents would be led around the central shield, and thus the distance between the end of the effective decay path and the detectors could be reduced, with a consequent advantage in the neutrino flux.